



Effects of the surface layer structure of the heterogeneous ion-exchange membranes on their impedance



Daniel Golubenko, Yulia Karavanova, Andrey Yaroslavltssev *

Kurnakov Institute of General and Inorganic Chemistry of RAS, 31 Leninsky prospect, Moscow, Russia

ARTICLE INFO

Article history:

Received 14 May 2016

Received in revised form 13 July 2016

Accepted 15 July 2016

Available online 17 July 2016

Keywords:

Ion exchange membranes

Impedance spectroscopy

Surface heterogeneity

Equivalent electrical circuit

Polarization resistance

ABSTRACT

Experimental details of measuring the impedance of heterogeneous membranes by the contact method with graphite electrodes in an aqueous medium were considered. It was shown that the inductive and capacitive components of the cell impedance lead to overestimation of the ionic resistance of heterogeneous and homogeneous membranes by 9% and 27%, respectively. Considering the physicochemical structure of heterogeneous membranes and proceeding from the Randles circuit, an equivalent electrical circuit capable of correct impedance description for heterogeneous membranes was proposed. The pressure effect on the membrane impedance was studied. An increase in the pressure on the electrodes to 2 MPa was shown to result in a considerable increase in the polarization resistance of heterogeneous membranes and decrease in the ionic resistance.

© 2016 Published by Elsevier B.V.

1. Introduction

Membrane technologies are utilized in many branches of industry. Approaches that use ion exchange membranes or membranes with an active ion exchange layer are among the most demanded ones. These types of membranes are widely used in water desalting [1,2] for alternative power generation [3,4] and for electrosynthesis [5,6].

Homogeneous membranes, which represent uniform ion exchange resin films, are used most often in fuel cells and in electrosynthesis. The manufacture of these membranes is complicated, and, therefore, they are expensive. Desalting is performed using much less expensive heterogeneous membranes, which are composites consisting of a reinforced polyethylene or polypropylene matrix and an ion exchange resin as a filler [7]. The surface of these membranes is made of an inert polymer by 80–90%, while the volume fraction of the ion exchange resin is about 60% [8]. The presence of a considerable amount of a non-conductive phase on the surface of heterogeneous ion exchange membranes was demonstrated by electron microscopy and by electrochemical methods [9,10].

Ionic conductivity, which is important for practical application of ion exchange membranes, is measured by impedance spectroscopy. Methods for measuring ionic conductivity of membranes can be classified into contact and difference ones. Contact methods imply the direct attachment of electrodes to the membrane; however, this brings about uncertainty in the membrane/electrode contact impedance, solution of which requires additional effort [11,12]. The contact measurement of

the impedance of heterogeneous membranes is often performed in a mercury cell [13]. However, this method has some considerable drawbacks. At the time of measurement the membrane can be partially dehydrated [14], which is especially true for thin samples. Toxic mercury, which contaminates the membrane surface, is used as electrodes. Therefore, other types of electrodes and non-destructive measurements in contact with water could provide a good alternative.

This paper describes the details of measuring the impedance of heterogeneous membranes by the contact method with graphite electrodes in water. The effects of pressure on the electrodes and the surface inhomogeneity on the impedance of heterogeneous membranes are considered. The trends listed above are analyzed both qualitatively and quantitatively using the equivalent circuit method. For homogeneous membranes, the equivalent electrical circuit (EEC) was based on the Randles circuit, which we modified to obtain the EEC for heterogeneous membranes [15].

2. Experimental

2.1. Materials

We used heterogeneous membranes, MC-40 and AMEX, and a homogeneous membrane, MF-4SC. The membrane composition, manufacturers and other characteristics are summarized in Table 1.

2.2. Equipment and configuration of the measuring cell

The measuring cell used in our work was a symmetric system of a membrane, graphite electrodes, current-carrying copper electrodes,

* Corresponding author.

E-mail address: yaroslav@igic.ras.ru (A. Yaroslavltssev).

Table 1
Characteristics of the ion exchange membranes.

| Membrane | MF-4SC | MC-40 | AMEX |
|--|--------------------------------|----------------------------------|---------------------------------|
| Manufacturer | JSC Plastpolymer | JSC Shchekinoazot | JSC Mega |
| Production method | Extrusion | Hot pressing | |
| Functional groups | R-SO ₃ ⁻ | | R'-NR ₃ ⁺ |
| Polymer base of the ion exchange resin | Perfluorinated copolymer | Styrene divinylbenzene copolymer | |
| Type | Homogeneous | Heterogeneous | |
| Thickness in the wet state, μm | 100 | 510 | 770 |
| Inert base | — | Polyethylene | |

and 10-mm thick organic glass plates anchored by a spring assembly to maintain a constant pressure. The whole system was immersed in deionized water to maintain a 100% humidity.

The impedance was measured using a 2B-1 impedance meter in the frequency range of 1–6 · 10⁶ Hz and an AC voltage of 100 mV. The data were approximated using a ZView program package. The membrane thickness was measured by a Mitutoyo micrometer, series 293. Deionized water was obtained using a Millipore water treatment setup (18.2 MΩ · cm).

2.3. Procedures

All cation exchange and anion exchange membranes were conditioned according to standard procedures [16]. For conversion to the sodium and chloride forms, membranes were successively kept in 0.1 M NaCl solutions for an hour and washed with deionized water three times. For removing the surface layer, membranes were polished on both sides in the wet state with the G44H sandpaper (grit size P1200) and, after polishing, the treated membrane was washed in deionized water.

The force by which the spring pressed on the cell was found using a force gauge, one end of the spring being secured and the other end being attached to the gauge. The spring assembly was stretched to the measuring cell size. The measured force was 49 N and remained constant for several hours. The pressure on the electrodes was changed by varying the electrode surface area and calculated as the ratio of the applied force to the electrode surface area.

The membrane impedance Z was analyzed in two ways, namely, as the Nyquist plots representing the dependence of the impedance complex number $\text{Im}(Z)$ on the real part $\text{Re}(Z)$ and as Bode phase plot representing the dependences of the phase angle θ between the ac voltage applied and the ac current arising in the system on the logarithm of the ac current frequency $\log(f)$.

At frequencies above 100 kHz, the true impedance value can be distorted by the impedances of the connecting wires and the measuring cell. The inductive and capacitive components for the cell were found by measuring the impedance of short electrodes and electrodes separated by an insulator of the same thickness as the membrane, and the result was subtracted from the obtained membrane impedance according to [17] using formula (1).

$$Z_{\text{true}} = (Z_m - Z_s) / (1 - Z_m / Z_o) \quad (1)$$

where Z_{true} is the true membrane impedance, Z_s is the short-cell impedance, Z_o is the open-cell impedance, and Z_m is the measured impedance value.

3. Equivalent electrical circuit of a homogeneous membrane

There is no common approach to the design of equivalent electrical circuits (EEC) describing the impedance Nyquist plots for ion exchange membranes. This is largely caused by different methods for impedance measurement and, as a consequence, basically different resistances, capacitances, and inductances formed in the system. The greatest progress was made in the modeling of ion-exchange membrane impedance obtained by difference method, where the three-layer system consisted of a cation-exchange membrane and two adjoining diffusion layers was studied [18,19]. However, it is difficult to describe the contact impedance of membrane with the help of the above approaches without adjacent solutions obtained with ideally polarizable electrode. In order to compose an EEC for contact measurements for a heterogeneous membrane, we started out from the Randles circuit adjusted to a homogeneous medium with mainly ionic charge carriers [15] (Fig. 1a).

This circuit (Fig. 1a) reflects rather comprehensively the physical scheme of the cell. The ionic resistance of the sample is reflected by the resistive element (R_m), while the processes of electrical double layer (EDL) charge/discharge at the membrane – electrode boundary, dielectric relaxation of the sample, and diffusion toward the electrodes are represented by the capacitors C_d and C_g and by the Warburg element (W), respectively.

However, even for a model system, the EEC of a homogeneous medium with mainly ionic charge carriers (Fig. 1a) may lead to a faulty interpretation of approximation of experimental data, depending on the relationship between the ion mobility and concentration [15], because the equivalent circuit approach is not sufficiently rigorous. In practice, the behavior of the membrane is not ideal, which is related to the physicochemical inhomogeneity of both the test material bulk and the electrode/sample interface [20,21]. This brings about a poor approximation of experimental data.

Therefore, the electrode capacitor C_d and the Warburg element W are usually replaced by constant phase elements (CPEs) (Fig. 1b), whose impedance is determined from formula (2), or, alternatively, dispersion equations are used to find the relaxation time spectrum [22]. It is noteworthy that the “apparent” R_m value includes the contact resistance, which is determined by the quality of the contact between

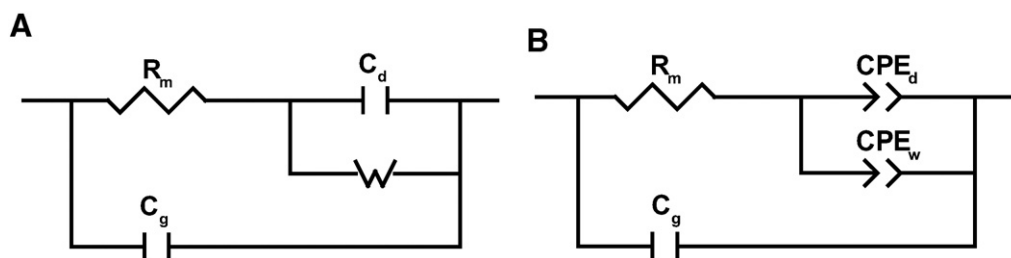


Fig. 1. (a) EEC for a conductor with predominantly ionic conduction, (b) EEC for a homogeneous membrane used in this work. (The ideal capacitor and the Warburg element were replaced by constant phase elements).

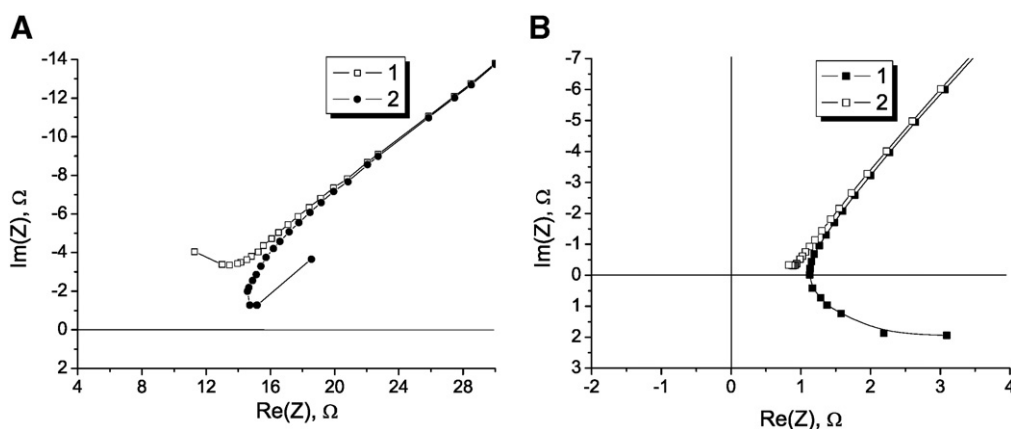


Fig. 2. High-frequency parts of the Nyquist plots for the homogeneous MF-4SC membrane (a) and heterogeneous MC-40 membrane (b) before (1) and after (2) the impedance correction.

the electrode and the membrane and may be the major part of R_m [11, 23,24].

$$Z = \frac{1}{T(i2\pi f)^n} \quad (2)$$

where i is the imaginary unit, f is the current frequency, T is the CPE characteristics corresponding to the capacity of the ideal capacitor if $n = 1$, to the reciprocal of the Warburg constant equal to $1/T$ if $n = 0.5$, and to the reciprocal of the resistance of the resistor equal to $1/T$ if $n = 0$.

4. Results

4.1. Impedance corrections

The impedance of thin films determined by the contact method is markedly distorted in the high-frequency region because of the inductive and capacitive cell impedance components [17]. For $\sim 500 \mu\text{m}$ -thick heterogeneous membranes, a correction for the inductive component of the error is sufficient for obtaining a high-quality Nyquist plot at high frequency. For $\sim 100 \mu\text{m}$ and less thick homogeneous membranes, for correct Nyquist plot to be obtained, it is necessary also to take into account the capacitive component of the cell impedance. Taking account of the above factors leads to substantial changes in the overall form of the high-frequency parts of Nyquist plots (Fig. 2). For example, after the correction, the ionic resistance is 21% lower for the

homogeneous MF-4SC membrane and 10% lower for the heterogeneous MC-40 membrane.

4.2. EEC of a heterogeneous membrane

Analysis of the Bode phase plots (Fig. 3a) of homogeneous and heterogeneous membranes distinguishes a low-frequency region (0.1–100 Hz) in which the phase angles for both types of membranes are equal and are about 25° – 30° and the high-frequency region (10^2 – 10^6 Hz) in which the membrane behaviors are considerably different. A similar situation was observed in [25] where the charge/discharge of the electrical double layer (EDL) in the graphite/electrolyte solution system took place at phase angles much smaller than the theoretically substantiated value of 90° , because of the presence of surface inhomogeneity of graphite electrodes. In our case, not only the electrode but also the electrolyte (membrane) can be inhomogeneous. The inhomogeneity is clearly seen in the micrograph of the heterogeneous MC-40 membrane surface (Fig. 3b). The major part of the surface is formed by polyethylene, while the ion exchanger is exposed to the surface, thus deteriorating the polyethylene integrity. A fragment of the reinforcing net can also be seen in the image (Fig. 3b).

Thus, the high-frequency part of the Bode phase plot corresponds to the EDL charge/discharge at the membrane/electrode interface, the substantial differences between homogeneous and heterogeneous membranes in this region (Fig. 3a) being related exactly to the surface structure details. The decrease in the phase angle for heterogeneous membranes attests to the presence of pronounced inhomogeneity,

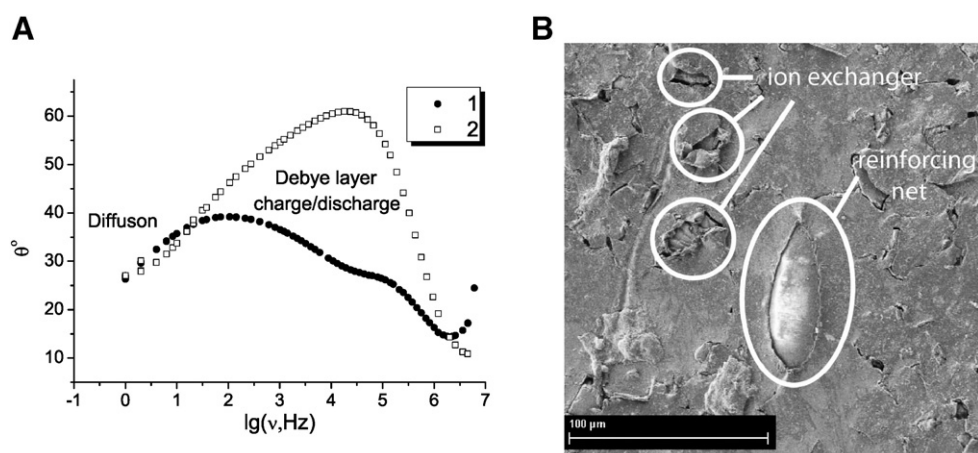


Fig. 3. Bode phase plots (a) of the heterogeneous MC-40 membrane (1) and homogeneous MF-4SC membrane (2) and electron micrograph (b) of the heterogeneous MC-40 membrane surface (the color marks the reinforcing net fragment exposed to the surface).

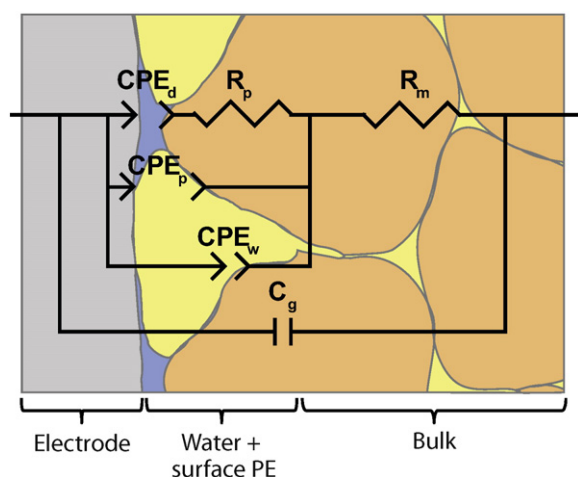


Fig. 4. Circuit of the heterogeneous membrane surface and its EEC used in this study.

which may be both physical (roughness) and chemical (alternation of the ion exchanger with the surface polyethylene).

The above-listed physicochemical phenomena can be reflected in the equivalent electrical circuit presented in Fig. 4. The presence of 10 to 20 μm -thick non-conductive polyethylene sections in the heterogeneous membrane — electrode system gives rise to two electrode EDLs in the Randles circuit, which are shown in the EEC as constant phase elements CPE_d and CPE_p (Fig. 4). In one EDL, the electrolyte is separated from the electrode by a thin film of the solution, which determines the system contact resistance. In the second EDL, a polyethylene layer occurs between the ions and the electrode. To approach the electrode, the ions must travel an additional distance, which is reflected by the presence of the resistor R_p (polarization resistance). The physical meaning of CPE_w , R_m and C_g is the same as in the EEC for the homogeneous membrane (Fig. 1b).

4.3. Approximation of the impedance of homogeneous and heterogeneous membranes using the proposed EEC

The introduction of CPE into the EEC of homogeneous membranes has markedly improved the quality of approximation (Fig. 5). The EEC of heterogeneous membranes equally well describes their impedance over the whole range of measurements (Fig. 6), which distinguishes our circuit from that used previously [23] where similar phenomena were observed for other objects.

Among the obtained approximation parameters, the parameter n for homogeneous membranes is about 0.7–0.8, while for electrolyte

solutions it varies in the range of 1–0.9, depending on the surface characteristics of graphite electrodes [21]. The decrease in this parameter at tests to a considerable contribution of the homogeneous membrane/electrode contact to the capacity dispersion (Table 2). For the heterogeneous MC-40 and AMEX membranes, the CPE capacity dispersion is even higher ($n = 0.6$ –0.7). This is reflected in the Bode phase plot as low phase angles of the EDL charge/discharge process compared with the same values for a homogeneous membrane (Table 2).

The obtained values for the bulk ionic resistance of the heterogeneous MC-40 membrane (Table 2) is in good agreement with the values determined in the contact mercury cell [13]. The polarization resistance R_p for the highest pressure exerted on the electrodes is 3–5 times higher than the corresponding R_m values (Table 2) and depends appreciably on the impedance approximation at low frequency. Apparently, higher surface homogeneity of the AMEX membrane (Fig. 7a, b) compared with MC-40 leads to much lower polarization resistances (Table 2).

In order to prove that the elements (R_p – CPE_p) refer to the surface layer, this layer of the MC-40 membrane was removed by sandpaper. The electron micrographs of the MC-40 membrane surface after the treatment (Fig. 7c) clearly reveal the destruction of the polyethylene film.

The removal of the surface layer induces changes in the membrane impedance, in particular, both the additional semicircle and the high-frequency peak disappear from the Nyquist plots and the Bode phase plots of the MC-40 membrane (Fig. 8). Finally, the impedance Nyquist plot of MC-40 approaches that of a homogeneous membrane. Also, owing to the reduced influence of the surface layer, the EEC parameters of the heterogeneous membrane (Table 2, treated MC-40) related to the surface layer (R_p , CPE_p –T) cannot be determined to a sufficient accuracy that indicative of their uselessness [25].

4.4. Change in the impedance of a heterogeneous membrane with pressure change

To the best of our knowledge for heterogeneous membranes this is the first attempt to investigate the dependence of the impedance on the pressure on the electrodes. The effect of pressure on the impedance of homogeneous membranes measured by contact methods has been thoroughly studied. By increasing pressure, it is possible to decrease the contact resistance R_{ct} , which increases the “apparent” bulk ionic resistance of the membrane. For example, in [11], the ionic resistance of the homogeneous Nafion® membranes reached a constant value at $7.6 \cdot 10^6$ Pa. In our experiments with the MF-4SC membrane, a plateau is already reached at $0.5 \cdot 10^6$ Pa, which is probably attributable to a different nature of electrodes. The graphite foil we use is likely to provide a better contact at the same pressure.

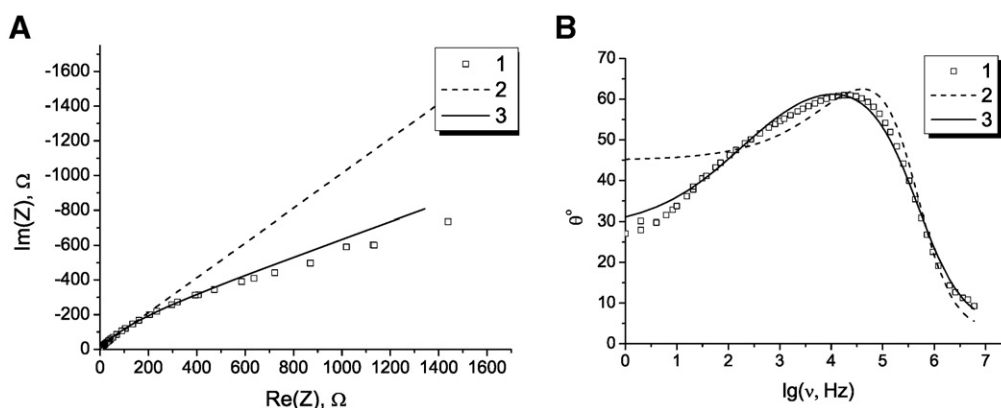


Fig. 5. Approximation of the Nyquist plots (a) and Bode phase plots (b) of a homogeneous MF-4SC membrane by means of equivalent circuits shown in Fig. 1a (1) and b (2). The dots correspond to experimental values.

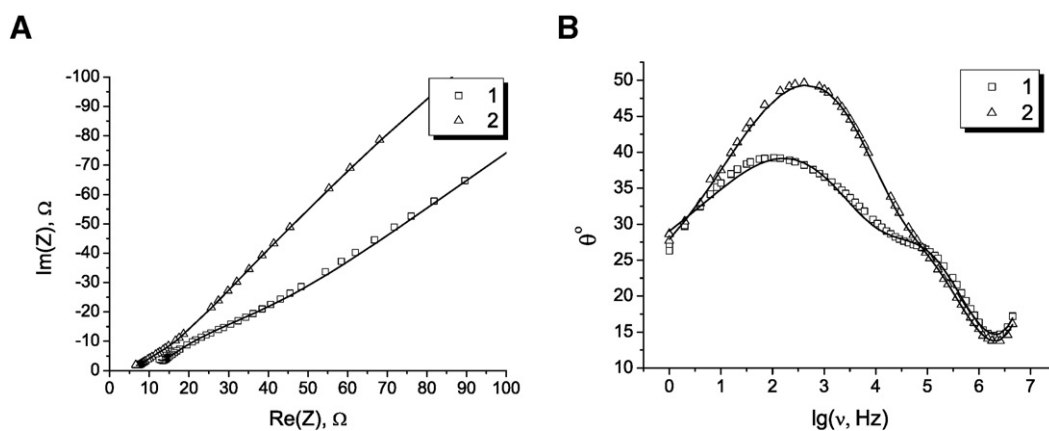


Fig. 6. Approximation of the Nyquist plots (a) and Bode phase plots (b) for the heterogeneous MC-40 (1) and AMEX (2) membranes. The dots correspond to experimental values. The lines imply the approximating curves. The approximation parameters are summarized in Table 2.

Table 2

Nyquist plot approximation parameters for the membranes. The pressure exerted on the electrodes is $1.96 \cdot 10^6$ Pa.

| EEC parameter | MC-40 | treated MC-40 | MF4-SK | AMEX |
|--|--------------------------------|---------------------------|----------------------|----------------------|
| $R_m, \Omega \cdot \text{cm}^2$ | 12.5 ± 0.5 | 12.1 ± 0.6 | 0.78 ± 0.05 | 6.7 ± 0.1 |
| $R_p, \Omega \cdot \text{cm}^2$ | 51 ± 2 | 8 ± 16 | — | 21 |
| $\text{CPE1-T}, \text{F} \cdot \text{cm}^{-2}$ | $5.25 \cdot 10^{-5}$ | $2 \cdot 10^{-6}$ | $1.24 \cdot 10^{-5}$ | $1.27 \cdot 10^{-5}$ |
| CPE1-n | 0.68 | 0.76 | 0.773 | 0.67 |
| $\text{CPE2-T}, \text{F} \cdot \text{cm}^{-2}$ | $(4.8 \pm 0.05) \cdot 10^{-5}$ | $(4 \pm 2) \cdot 10^{-5}$ | — | $1.9 \cdot 10^{-5}$ |
| CPE2-n | 0.562 | 0.52 | — | 0.66 |
| $\text{CPEw-T}, \text{F} \cdot \text{cm}^{-2}$ | $2.5 \cdot 10^{-4}$ | $2.4 \cdot 10^{-4}$ | $3.4 \cdot 10^{-4}$ | $2.4 \cdot 10^{-4}$ |
| CPEw-n | 0.22 | 0.27 | 0.312 | 0.21 |
| $\text{Cg}, \text{F} \cdot \text{cm}^{-2}$ | $5 \cdot 10^{-10}$ | $6 \cdot 10^{-10}$ | $4 \cdot 10^{-10}$ | $9 \cdot 10^{-10}$ |

In the case of heterogeneous membranes, the pressure dependence of R_m is similar (Fig. 9a) but it can have additional causes. Heterogeneous membrane structure tends to have meso- and macropores between the ion exchanger grains and the inert polymer matrix [26]. By applying pressure, we compact the membrane, thus improving the contact between the ion exchanger particles, and this may decrease in the resistance. Indeed, during the impedance measurement at a maximum pressure, the membrane thickness decreases by 7%. The conductivity of the MC-40 membrane at high pressure can reach 4.8 mS/cm, thus approaching the conductivity of ion exchanger grains, which is likely to be similar to the conductivity of the “gel” phase (5.2 mS/cm) [13].

Meanwhile, the low-pressure conductivity of the membrane is close to that in contact-mercury cell for dilute solutions. These facts suggest that parameters of the microheterogeneous model of membranes [26] can be determined from the dependence of the membrane resistance on the electrodes pressure.

Apart from the decrease in the bulk resistance, pressure rise induces an increase in the surface component (Fig. 9b). Meanwhile, the expected improvement of the electrode/membrane contact, as observed for homogeneous membranes [23], does not take place. Presumably, increase in the pressure exerted on the electrodes results in forcing-in of the ion exchanger particles and surface exposure of the more plastic,

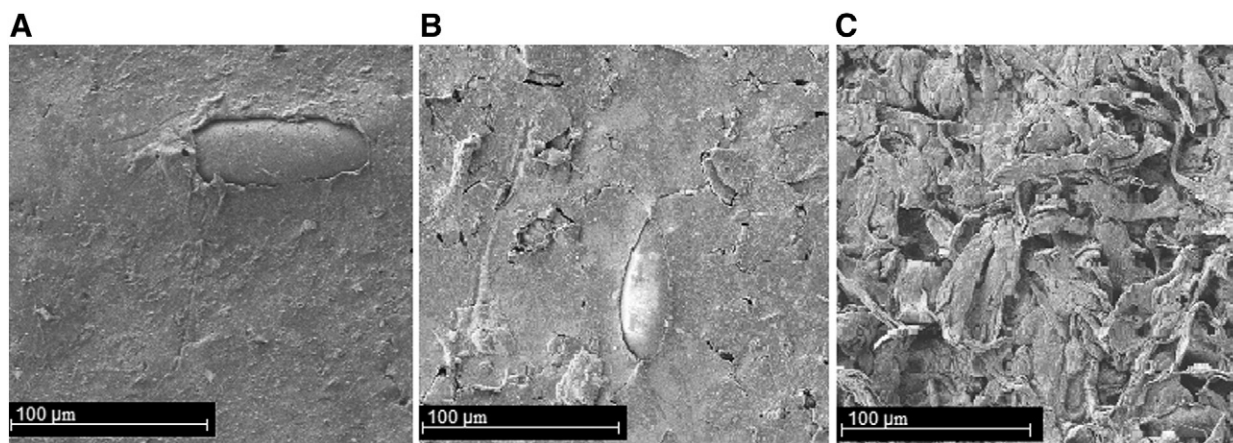


Fig. 7. Electron micrographs of the surfaces of initial MC-40 (a) and AMEX (b) membranes and treated MC-40 membrane (c).

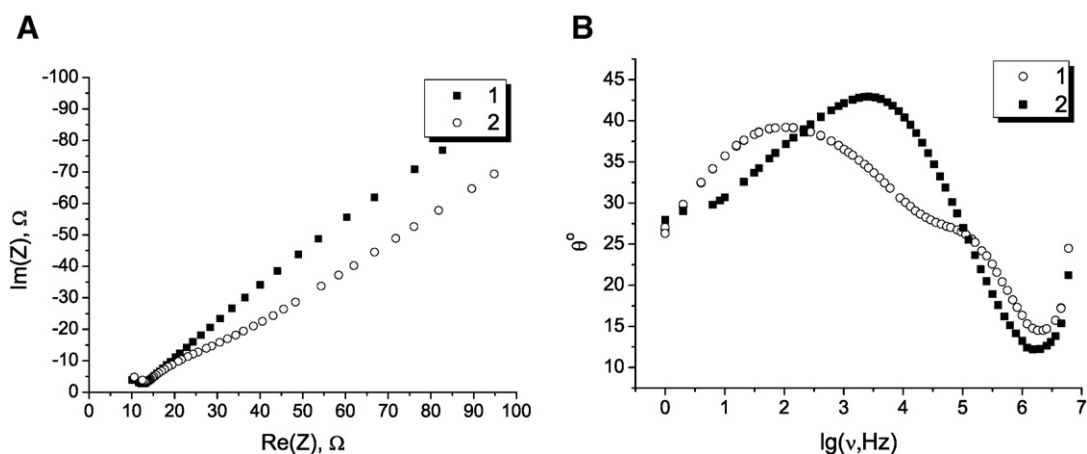


Fig. 8. Nyquist plots (a) and Bode phase plots (b) of the MC-40 membrane before (1) and after (2) removal of the surface layer. The pressure on the electrodes is $1.96 \cdot 10^6$ Pa; the approximation parameters are summarized in Table 2.

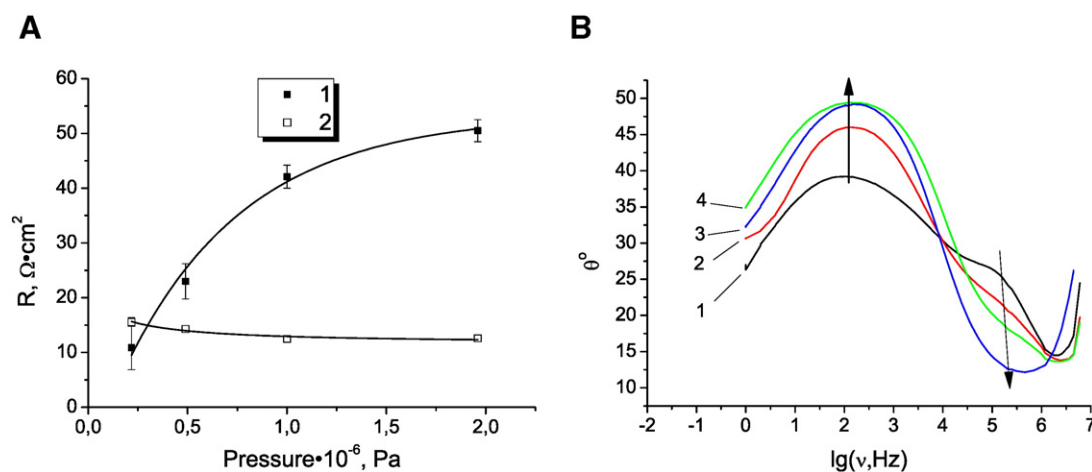


Fig. 9. Surface R_p (1) and bulk R_m (2) resistance of the MC-40 membrane vs. electrode pressure (a) and the Bode phase plots for membrane under different electrode pressure (b). (1) 1.96 MPa, (2) 1 MPa, (3) 0.22 MPa, (4) 0.5 MPa.

non-conductive, polyethylene phase (Fig. 10). This enhances the electrode/membrane contact, which may be one of the reasons for decrease in the bulk resistance R_m . Simultaneously, the surface rearrangement results in increase in the polarization resistance R_p (Fig. 9a).

This process progresses with time (Fig. 11). The polarization resistance increases linearly, whereas the bulk resistance R_m remains

invariable, being also indicative of the rearrangement of surface layers under the action of electrode pressure.

The above-described phenomenon may take place in real industrial processes. In an electrodeionization facility, the space between the membranes is tightly filled with ion exchanger grains [27]. The ion exchanger exerts high pressure on the membrane at the contact site and

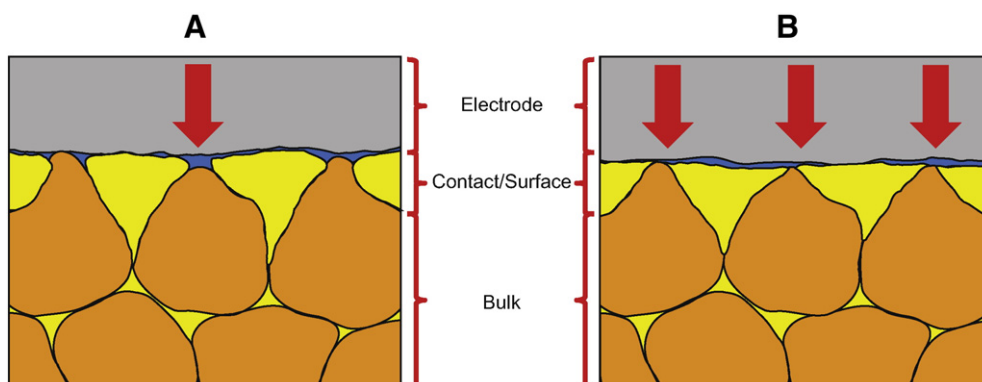


Fig. 10. Pressure effect on the membrane surface morphology (a is low pressure; b is high pressure of electrodes on the membrane).

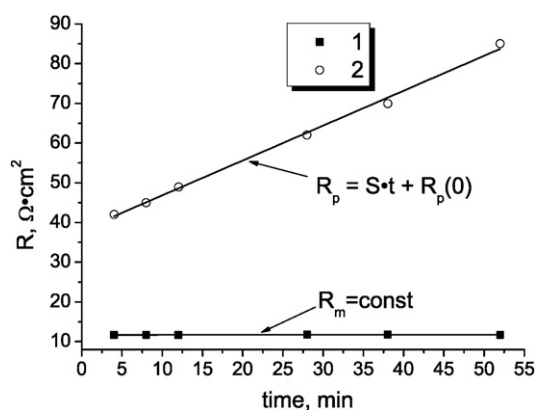


Fig. 11. Change in the polarization (1) and bulk (2) resistance with time for the heterogeneous MC-40 membrane at a pressure of $1 \cdot 10^6$ Pa, $S = 0.8$, $\Omega \cdot \text{cm}^2/\text{min}$, $R_p(0) = 42 \Omega \cdot \text{cm}^2$.

thus it can press the ion exchanger particles of heterogeneous membrane below the surface and, as a consequence, increase the internal polarization resistance, thus decreasing the energy efficiency of the facility.

5. Conclusions

It was shown that the polarization resistance of heterogeneous membranes can be created by not only physical inhomogeneity of the contact but also by the heterogeneous structure itself. The proposed model of the surface structure for heterogeneous membranes, which takes into account the presence of non-conductive polyethylene sites on the surface, can serve to compose an equivalent electrical circuit describing the membrane behavior in the range of $1\text{--}6 \cdot 10^6$ Hz. The proposed EEC interpretation accounts for the dependence of the membrane impedance on the pressure exerted on the electrodes and for specific features of their phase diagrams and impedance Nyquist plots. In relation to heterogeneous ion exchange membranes, it was demonstrated that by measuring the bulk resistance of the membrane under the electrode pressure, it is possible to determine microheterogeneous model parameters and to study the surface homogeneity.

Acknowledgment

This work was supported by the Russian Science Foundation (Project No. 16-13-00127).

References

- [1] H. Strathmann, A. Grabowski, G. Eigenberger, Ion-exchange membranes in the chemical process industry, *Ind. Eng. Chem. Res.* 52 (2013) 10364–10379, <http://dx.doi.org/10.1021/ie4002102>.
- [2] T. Sata, *Ion Exchange Membranes - Preparation, Characterization, Modification and Application*, The Royal Society of Chemistry, Cambridge, 2004.
- [3] J.G. Hong, B. Zhang, S. Glabman, N. Uzal, X. Dou, H. Zhang, et al., Potential ion exchange membranes and system performance in reverse electrodialysis for power generation: a review, *J. Membr. Sci.* 486 (2015) 71–88, <http://dx.doi.org/10.1016/j.memsci.2015.02.039>.
- [4] G. Pourcelly, Membranes for low and medium temperature fuel cells. State-of-the-art and new trends, *Pet. Chem.* 51 (2011) 480–491, <http://dx.doi.org/10.1134/S0965544111070103>.
- [5] L.M. Inanuddin, M. Luqman (Eds.), *Ion Exchange Technology I - Theory and Materials*, Springer, London, 2012.
- [6] E.Y. Safronova, A.B. Yaroslavtsev, Prospects of Practical Application of Hybrid Membranes, 6, *Membrany i membrannye tekhnologii*, 2016 3–16 (in Russian) Смолы ионообменные Катиониты, (n.d.).
- [7] A.B. Yaroslavtsev, V.V. Nikonenko, Ion-exchange membrane materials: Properties, modification, and practical application, *Nanotechnol. Russ.* 4 (2009) 137–159, <http://dx.doi.org/10.1134/S199507800903001X>.
- [8] J. Krivčík, J. Vláďařová, J. Hadravá, A. Černín, L. Brožová, The effect of an organic ion-exchange resin on properties of heterogeneous ion-exchange membrane, *Desalin. Water Treat.* 14 (2010) 179–184, <http://dx.doi.org/10.5004/dwt.2010.1025>.
- [9] E. Volodina, N. Pismenskaya, V. Nikonenko, C. Larchet, G. Pourcelly, Ion transfer across ion-exchange membranes with homogeneous and heterogeneous surfaces, *J. Colloid Interface Sci.* 285 (2005) 247–258, <http://dx.doi.org/10.1016/j.jcis.2004.11.017>.
- [10] S. Mareev, A. Kozmai, V. Nikonenko, E. Belashova, G. Pourcelly, P. Sistat, Chronopotentiometry and impedancemetry of homogeneous and heterogeneous ion-exchange membranes, *Desalin. Water Treat.* 1–4 (2014), <http://dx.doi.org/10.1080/19443994.2014.981930>.
- [11] T. Soboleva, Z. Xie, Z. Shi, E. Tsang, T. Navessin, S. Holdcroft, Investigation of the through-plane impedance technique for evaluation of anisotropy of proton conducting polymer membranes, *J. Electroanal. Chem.* 622 (2008) 145–152, <http://dx.doi.org/10.1016/j.jelechem.2008.05.017>.
- [12] S. Park, J.-S. Yoo, Electrochemical impedance spectroscopy for better electrochemical measurements, *Anal. Chem.* 75 (2003) 455a–461a, <http://dx.doi.org/10.1021/ac0313973>.
- [13] L.V. Karpenko-Jereb, A.-M. Kelterer, N.P. Berezina, A.V. Pimenov, Conductometric and computational study of cationic polymer membranes in H^+ and Na^+ -forms at various hydration levels, *J. Membr. Sci.* 444 (2013) 127–138, <http://dx.doi.org/10.1016/j.memsci.2013.05.012>.
- [14] L.V. Karpenko, O.A. Demina, G.A. Dvorkina, S.B. Parshikov, C. Larchet, B. Auclair, et al., Comparative study of methods used for the determination of Electroconductivity of ion-exchange membranes, *Russ. J. Electrochem.* 37 (2001) 287–293, <http://dx.doi.org/10.1023/A:1009081431563>.
- [15] J. Jamnik, J. Maier, S. Pejovnik, A powerful electrical network model for the impedance of mixed conductors, *Electrochim. Acta* 44 (1999) 4139–4145, [http://dx.doi.org/10.1016/S0013-4686\(99\)00128-0](http://dx.doi.org/10.1016/S0013-4686(99)00128-0).
- [16] GOST 17552-72; GOST 17553-72; GOST 17554-72 (State Standard, Russia)
- [17] A.K. Ivanov-Shiz, I.V. Murin, *Solid State Ionics I*, Publishing house of SPU, St. Petersburg, 2000 (in Russian).
- [18] V.V. Nikonenko, A.E. Kozmai, Electrical equivalent circuit of an ion-exchange membrane system, *Electrochim. Acta* 56 (2011) 1262–1269, <http://dx.doi.org/10.1016/j.electacta.2010.10.094>.
- [19] A.A. Moya, J.A. Moleón, Study of the electrical properties of bi-layer ion-exchange membrane systems, *J. Electroanal. Chem.* 647 (2010) 53–59, <http://dx.doi.org/10.1016/j.jelechem.2010.05.011>.
- [20] W.H. Molder, J.H. Sluyters, Tafel current at fractal electrodes, Connection With Admittance Spectra, 285, 1990, pp. 103–115, [http://dx.doi.org/10.1016/0022-0728\(90\)87113-X](http://dx.doi.org/10.1016/0022-0728(90)87113-X).
- [21] C.-H. Kim, S.-I. Pyun, J.-H. Kim, An investigation of the capacitance dispersion on the fractal carbon electrode with edge and basal orientations, *Electrochim. Acta* 48 (2003) 3455–3463, [http://dx.doi.org/10.1016/S0013-4686\(03\)00464-X](http://dx.doi.org/10.1016/S0013-4686(03)00464-X).
- [22] J. Ross Macdonald, Analysis of dispersed, conducting-system frequency-response data, *J. Non-Cryst. Solids* 197 (1996) 83–110, [http://dx.doi.org/10.1016/0022-3093\(95\)00618-4](http://dx.doi.org/10.1016/0022-3093(95)00618-4).
- [23] S.-H. Yun, S.-H. Shin, J.-Y. Lee, S.-J. Seo, S.-H. Oh, Y.-W. Choi, et al., Effect of pressure on through-plane proton conductivity of polymer electrolyte membranes, *J. Membr. Sci.* 417–418 (2012) 210–216, <http://dx.doi.org/10.1016/j.memsci.2012.06.041>.
- [24] C. Lee, H. Park, Y. Lee, R. Lee, Importance of proton conductivity measurement in polymer electrolyte membrane for fuel cell application, *Ind. Eng. Chem. Res.* 44 (2005) 7617–7626, <http://dx.doi.org/10.1021/ie0501172>.
- [25] E. Barsoukov, J.R. Macdonald, *Impedance Spectroscopy: Theory, Experiment, and Applications*, second ed. John Wiley & Sons, Inc., New Jersey, 2005.
- [26] N.P. Berezina, N.A. Kononenko, O.A. Dyomina, N.P. Gnusin, Characterization of ion-exchange membrane materials: properties vs structure, *Adv. Colloid Interf. Sci.* 139 (2008) 3–28, <http://dx.doi.org/10.1016/j.cis.2008.01.002>.
- [27] D.V. Golubenko, J. Krivčík, A.B. Yaroslavtsev, Evaluating the effectiveness of ion exchangers for the electrodeionization process, *Pet. Chem.* 55 (2015) 769–775, <http://dx.doi.org/10.1134/S0965544115100059>.